IFSCC 2025 full paper (IFSCC2025-452)

Skin aging ameliorated via the reprogramming energy metabolism by an NAMPT activator in senescent fibroblasts

Baolin Ge[1, *], Ying Wang[1, *], Jie Gu[1], Zhi Lv[1], Qilong Chen[1], Haojing Wang[1], Jingming Gao[2]

[1]Department of Research and Innovation, Shanghai Inoherb Cosmetics Co. Ltd., Shanghai, China.
2Department of Plastic and Reconstructive Surgery, Shanghai 9th People's Hospital, Shanghai Jiao Tong University School of Medicine, Shanghai, China.
*These authors contributed equally to this work

1. Introduction

Aging is a complex process that encompasses various hierarchical levels, from molecules to organ systems, which are also intricately interconnected [1]. Numerous studies employing cellular and mouse models have established strong links between metabolic regulation, cellular senescence, and organ aging [2-5]. The accumulation of senescent cells with age significantly contributes to both organ dysfunction and the overall organismal aging[6]. In contrast to normal cells that primarily generate large amounts of adenosine triphosphate (ATP) through oxidative phosphorylation (OXPHOS) under aerobic conditions [7,8]. senescent cells exhibit a shifted metabolic pattern characterized by excessive reliance on glycolysis, often resulting in only a net production of two ATP molecules [9]. This metabolic shift leads to ATP depletion and subsequent cellular dysfunction. Therefore, interventions that target metabolic regulation significantly influences the properties of senescent cells and help to ameliorate age-related diseases [10]. such as adipose tissue fibrosis [11,12], age-associated frailty [13]. Alzheimer's disease [14,15] and type II diabetes [16].

Skin aging is one of the most prominent external characteristics of biological aging, manifested by wrinkles [17]. epidermis thinning [18]. dermis thinning [17]. a decreased number of fibroblasts [19] and an imbalanced extracellular matrix (ECM) homeostasis [20]. This deterioration not only compromises the skin's barrier function for the whole body [21], but also accelerates aging phenotypes in other systemic organs due to the incorporation of various cell types in skin, including those from the nervous, immune, circulatory, and endocrine systems systems [22]. Similar to other organs, the significant contributors to skin aging are also cellular senescence [23] and metabolic dysfunction [24]. For instance, senescent fibroblasts demonstrate impaired mitochondrial function [25] and preferentially engage in glycolytic metabolism [26] even in the presence of abundant oxygen, ultimately leading to skin aging. Uncovering the mechanisms behind metabolic imbalance in skin cells and identifying potential interventions could provide effective strategies for combating skin aging.

Playing a central role in energy metabolism, nicotinamide adenine dinucleotide (NAD+) serves as an electron acceptor to form reduced NADH, which subsequently donates electrons to complex Ⅰ (NADH: ubiquinone oxidoreductase) in the inner mitochondrial membrane to support the electron transport chain during OXPHOS process [8,27]. The

OXPHOS process ultimately generates nearly 34 ATP molecules through ATP synthase, significantly exceeding the amount produced during glycolysis [11]. Thus, the decreased NAD+ level during aging is considered take charge of impaired OXPHOS and many degenerative diseases [28]. Nicotinamide phosphoribosyltransferase (NAMPT) is a key rate-limiting enzyme in the nicotinamide adenine dinucleotide (NAD+) salvage pathway and distributes in various tissues, facilitating the conversion of nicotinamide (NAM) to nicotinamide mononucleotide (NMN), an NAD+ precursor. Regulated by circadian genes, NAMPT levels in various tissues and plasma decline with age [29,30]. resulting in NAD+ depletion and metabolic dysfunction [31]. Small molecule activators of NAMPT can delay the onset of neurodegenerative disorders [32], while overexpression of the NAMPT activity has been shown to extend the lifespan of organisms [29,33], at least in part by boosting NAD+ levels.

Despite there have been extensive research on NAMPT in the context of aging in other organs, the relationship between NAMPT, metabolic patterns and skin aging remains unclear, with existing studies primarily focusing on NAD+ precursors [34,35]. Herein, we aimed to evaluate the effects of a small molecule NAMPT activator, NAT, on skin aging. In vitro evidence demonstrated that upon activation of NAMPT expression by NAT, the energy metabolism of senescent fibroblasts was reprogrammed by downregulating glycolytic enzyme, pyruvate kinase M1 (PKM1), and upregulating component of complex I, mitochondrially encoded NADH: ubiquinone oxidoreductase core subunit 1 (mt-ND1). The shift from glycolysis to OXPHOS facilitated amelioration of mitochondrial dysfunction, ineffective ATP production, extracellular matrix deterioration. Our results provide evidence that targeting NAMPT to reprogram energy metabolism may serve as a promising therapy for skin aging, potentially offering reparative benefits for aged individuals.

2. Materials and Methods

Cell culture

Primary human dermal fibroblasts (HDF), generously gifted by the Ninth People's Hospital of the Shanghai Jiao Tong University School of Medicine, were used in this study, which was approved by the Medical Ethical Committee and conducted in accordance with the Declaration of Helsinki. HDF were cultured in DMEM supplemented with 15% FBS, 1% p/s (complete media), and maintained at 37 °C in a humidified atmosphere of 5% CO_2 incubator (Forma Steri-Cycle i160, Thermo Fisher Scientific, Waltham, MA, USA). Subsequently, upon reaching approximately 80% confluence, HDF were passaged and allowed to proliferate in complete culture medium which was refreshed every 2 days. All experiments were performed using cells between passages 3 and 8.

Cell viability assay

The primary fibroblasts have been also used to investigate cellular senescence induced by DNA damage. The proliferation and viability of senescent fibroblasts was evaluated with a Cell Counting Kit-8 (CCK-8; M4839, AbMole, Houston, TX, USA) according to the manufacturer's instructions. Briefly, cells were seeded in 96-well plates (3599, Corning, CA, USA) with 8×10^3 cells/well, the culture medium was discarded and replaced by fresh medium containing 25 μM etoposide (ETO) or without ETO. After incubation, cells were cultured with the drug administration groups for 24 hours at 37 °C in 5% CO_2. Then, the medium was removed, cells were washed using DPBS, then 100 μL medium containing 10% CCK-8 reagents was added to each well and incubated for 2 hours in a 5%

CO_2 atmosphere at 37 °C without light. At last, absorbance was measured at 450 nm using a SpectraMaxM2 microplate reader (Molecular Devices LLC, CA, USA)

RNA isolation and RT-qPCR

Total RNA was extracted using the *SteadyPure* Universal RNA Extraction Kit (ACCURATE Biotechnology (Hunan) Co., Ltd，Changsha，China) following manufacturer's instructions. RNA concentrations were measured using a micro-spectrophotometry (NanoDrop2000, Thermo Fisher Scientific, Waltham, MA, USA). The extracted mRNA was reverse transcribed into cDNA using the *Evo M-MLV* RT Premix for qPCR Kit (ACCURATE Biotechnology (Hunan Co., Ltd，Changsha，China) in accordance with the manufacturer's guidelines. The relative expression levels of detected genes were quantified utilizing the SYBR Green Premix *Pro Taq* HS qPCR Kit（Rox Plus, ACCURATE Biotechnology, Huna Co., Ltd，Changsha，China) by the Applied Biosystems® QuantStudio™ 6 Flex Real-Time PCR System (Life Technologies, Waltham, MA, USA). Data analysis was conducted using the $2^{-\Delta\Delta Ct}$ method, with GAPDH serving as the housekeeping gene.

ELISA

Type I collagen in the cell-free supernatant was quantified using a PIP EIA kit (MK101, Takara Bio Inc., Shiga, Japan), while type III collagen was detected with Col III ELISA Kit (EH2866, FineTest, Wuhan, Hubei, China), following the manufacturers' instructions. In brief, the supernatant was centrifuged, and protein concentrations were quantified using an Enhanced BCA Protein Assay Kit (Beyotime, Shanghai, China). For the assay, 100 µL of labeled antibody was added to each well of the microtiter plate, followed by 20 µL of the test sample, and incubated at 37 °C for 3 hours. After incubation, the wells were repeatedly washed with 250 uL of washing solution for 4 times. Following the washing steps, substrate solution (TMBZ) was added to each well, evading the light preservation for 15 min at room temperature. The optical density (OD) at a wavelength of 450 nm was measured by SpectraMaxM2 microplate reader.

Western blotting

Fibroblast cells were washed three times with DPBS, and were lysed using RIPA Lysis Buffer (abs9229, absin, Shanghai, China). The concentration of total protein was determined with Enhanced BCA Protein Assay Kit. Proteins were mixed with loading buffer and were boiled for 5 minutes. Subsequently, denatured proteins and protein standard marker were loaded onto 4.5% stacking polyacrylamide gel with 10% separating gel (EpiZyme Biotechnology, Shanghai, China). The PVDF membranes were soaked for 30 seconds at room temperature in methanol and loaded proteins were transferred to a PVDF membrane with transfer buffer at a constant current of 400 mA for 35 minutes. The PVDF membrane was blocked with 1x protein-free rapid blocking buffer for 10 minutes at room temperature, followed by incubation under constant agitation with primary antibodies overnight at 4 °C. After aspiration of the primary antibody, the blot was washed three times with TBST, followed by a 1-hour incubation at room temperature with donkey anti-rabbit antibody conjugated to horseradish peroxidase (HRP) (Solarbio, Beijing, China) at a 1:5000 dilution. The membrane was then washed 5 times with TBST, and target protein bands were visualized using the Ultrasensitive ECL Chemiluminescence Kit (Beyotime Biotechnology, Shanghai, China). Images were captured with the Tanon 5200 imaging system (Tanon, Shanghai, China). The density of each band was measured using ImageJ software (Wayne Rasband, Bethesda, MD, USA) and normalized to the corresponding housekeeping protein band density.

Cellular metabolism analysis

Measurement of intracellular ATP content

ATP content was measured using the ATP Assay Kit-Luminescence (CK18, Dojindo, Kumamoto, Japan) according to the manufacturer's instructions. In a white, flat-bottom 96-well microplate (3917, Corning, CA, USA), 100 µL of cell suspension was added to each well, followed by 100 µL of working solution. The plate was then placed in a SpectraMaxM2 microplate reader, set to 25 °C, for a 10-minute incubation. Luminescence (RLU) was subsequently detected to quantify ATP levels.

JC-1 fluorescent staining

JC-1, a fluorescent probe, was used to detect mitochondrial membrane potential (ΔΨm). The JC-1 MitoMP Detection Kit (MT09, Dojindo, Kumamoto, Japan) was employed, where a decrease in the red/green fluorescence intensity ratio indicates mitochondrial depolarization. Proliferating non-senescent and senescent fibroblasts were treated with NAT for 4 hours at 37 °C, followed by culture in fresh DMEM medium. The cells were incubated with JC-1 dye for 20 minutes in the dark. After complete aspiration of the dye and four successive washes with DPBS (3 minutes each), fibroblasts were visualized using a fluorescence microscope equipped with a 49.15MP cooled color camera (IX73, Olympus, Tokyo, Japan).

Mitochondrial ROS (mtROS) measurement

The levels of mtROS were measured using a MitoSOX Red mitochondrial superoxide assay kit (Beyotime, Shanghai, China) according to the manufacturer's instructions. MitoSOX Red is rapidly oxidized in the presence of mitochondrial superoxide, resulting in red fluorescence. The intensity of this fluorescence serves as an indicator of superoxide levels in mitochondria. After treatment with SoxUp, a positive control to induce superoxide production, NAT cells were incubated with 5 µM MitoSOX Red for 20 minutes and then washed with fresh medium. The red fluorescence signal was quantified using the Cytation5 cell imaging multimode microplate reader (BioTek, Winooski, VT, USA).

Cellular oxygen consumption quantification

The oxygen consumption rate (OCR) was measured at 37 °C using the Extracellular OCR Plate Assay Kit (E297, Dojindo, Kumamoto, Japan) according to the manufacturer's instructions. HDF cells were seeded into each well of a 96-well black plate with a clear flat bottom (3904, Corning, CA, USA) and cultured for 24 hours. The cells were then stimulated with 25 µM etoposide for 4 hours. After discarding the medium, fresh working solution containing NAT was added, and the cells were incubated at 37 °C for 30 minutes. Mineral oil was carefully added to each well to create an airtight seal. Fluorescence signals (excitation at 500 nm and emission at 636 nm) were recorded at 5-minute intervals using the Cytation5 cell imaging multimode microplate reader. OCR was calculated by analyzing the kinetic profiles derived from these measurements.

Statistical analysis

All results were presented as mean ± standard deviation (SD) of at least three independent replicates and indicated in the legends of the figures. Statistical analysis was performed with GraphPad Prism 9 (GraphPad Inc., San Diego, CA, USA) using equal variance student's t-test and one-way ANOVA with Tukey's multiple comparison analysis. Results in abnormal distribution were analyzed by nonparametric test. A p value < 0.05 was considered statistically significant

3. Results and Discussion

3.1 NAT ameliorated dysfunction of senescent fibroblasts

3.1.1 NAT enhanced cell viability and activated NAMPT of senescent fibroblasts

Initially, the effect of NAT was investigated on etoposide (ETO)-induced senescence in human dermal fibroblasts (HDFs) using a CCK-8 assay (Figure 1A). After 24 hours culture, NAT treatment (2 to 8 μM) significantly enhanced cell viability, showing the highest viability of 117%, but not in a dose-dependent manner. Conversely, 1 μM NAT exhibited no significant difference compared to the ETO-only group, while 16 μM NAT (NAT16) led to a marked decrease in viability, suggesting the potential cytotoxicity by high doses. These results indicated that NAT provides notable protection against DNA damage-induced HDF senescence, though the high concentration (16 μM) exhibited cytotoxicity.

Furthermore, RT-qPCR results (Figure 1B) showed that ETO dramatically down-regulated NAMPT mRNA expression by 1.7-fold change, indicating the depletion of NAMPT in senescent HDFs. NAT treatment significantly up-regulated NAMPT mRNA expression in senescent fibroblasts, with 2 μM NAT restoring NAMPT levels to that of the control group. Previous studies reported that NAMPT functioned as both an NAD-biosynthetic enzyme and as a cytokine or growth factor [35]. For example, NAMPT overexpression enhanced cell proliferation via TLR4/NF-κB/PLK4 pathway [36] and suppressed cell senescence in endothelial progenitor cells [37]. In addition, NAMPT is crucial for regulating the proliferation, differentiation, and self-renewal of neural stem/progenitor cells [38]. Based on these findings, we hypothesize that NAMPT also functions both as an NAD-biosynthetic enzyme and as a cytokine or growth factor to promote fibroblasts proliferation.

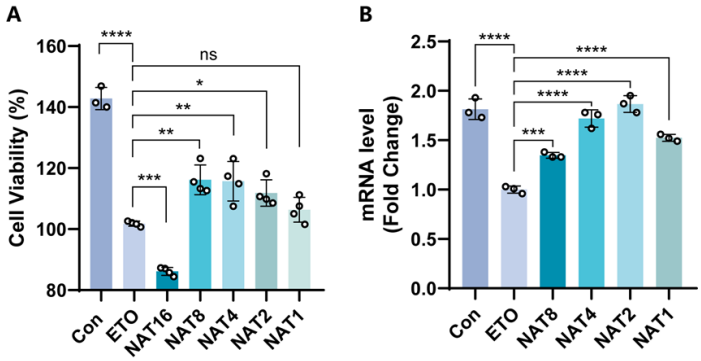

Figure 1. NAT increased cell viability and promoted NAMPT gene expression of senescent fibroblasts, inducted by ETO. (A) Cell cytotoxicity of senescent fibroblasts treated with 16 μM (NAT16), 8 μM (NAT8), 4 μM (NAT4), 2 μM (NAT2) or 1 μM (NAT1) NAT (normalized to ETO), n=4; (B) RT-qPCR analysis of mRNA expression changes of NAMPT in senescent fibroblasts (normalized to ETO), n=3. Data are represented as mean ± SD. *p <0.05, **p < 0.01, ***p < 0.001, ****p < 0.0001, ns, not significant, as determined by one-way ANOVA analyses with Tukey's post-hoc test for all comparisons.

3.1.2 NAT restored functions of senescent fibroblasts to remodel ECM

Collagen is the primary structural protein in the human dermal ECM [39] with type I collagen and type III collagen being crucial for skin strength and resilience [40]. In aged skin, collagen synthesis reduces, while matrix metalloproteinases (MMP) levels rise, leading to skin laxity and sagging [41]. To investigate the effects of DNA damage on collagen and MMP expression, we analyzed mRNA levels of COL1A1, COL3A1, MMP1, and HES1, as well as collagen types I and III protein synthesis in HDF cells after 24 hours of culture, using RT-qPCR and ELISA. Real-time PCR revealed a significant downregulation of COL1A1 and COL3A1 mRNA levels following ETO-induced

senescence, with COL1A1 expression reduced by 0.7-fold and COL3A1 by 1.8-fold, respectively (Figure2A). Interestingly, 2 μM of NAT treatment significantly upregulated mRNA expression levels of COL1A1 by 1.2-fold and COL3A1 by around 0.8-fold, compared to those of ETO induced senescent HDFs. Similarly, the Col I protein synthesis was elevated by approximately 19% and Col III protein was increased by 65% after 2 μM of NAT treatment, tested by ELISA assay (Figure 2B, 2C). Additionally, NAT markedly increased HES1 expression (Figure 2A), which previous studies have shown to mitigate cellular senescence in dermal fibroblasts [42]. While HES1 expression was reduced following DNA damage, NAT supplementation restored its levels. However, we also observed an increase in MMP1 mRNA expression after NAT treatment, indicating that NAT did not suppress MMP1 expression in aging fibroblasts following ETO induction. Overall, our findings suggest that NAT promotes collagen synthesis and helps restore the functionality of senescent fibroblasts, contributing to the remodeling of the extracellular matrix.

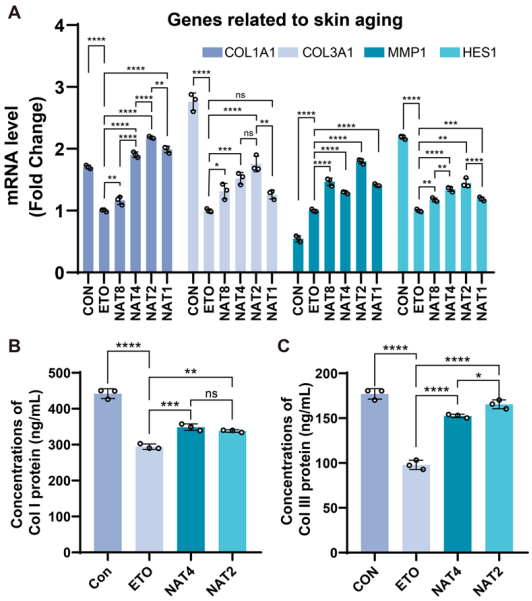

Figure 2. NAT restored functions of senescent fibroblasts to remodel ECM. (A) Relative mRNA expression changes of genes associated with skin aging, including collagen type I (COL1A1), collagen type III (COL3A1), matrix metallopeptidase 1 (MMP1) and Hes family BHLH transcription factor 1 (HES1), n=3; (B) The concentrations of collagen type I (Col I) protein secreted by fibroblasts, n=3; (C) The concentration of collagen type III (Col III) protein secreted by fibroblasts, n=3; Data are represented as mean ± SD. *p <0.05, **p < 0.01, ***p < 0.001, ****p < 0.0001, ns, not significant, as determined by one-way ANOVA analyses with Tukey's post-hoc test for all comparisons.

3.2 NAT reprogrammed energy metabolism and enhanced ATP production of senescent fibroblasts

Although senescent cells have been shown to exhibit a shift in energy metabolism toward glycolysis [9], they were also characterized by impaired mitophagy and autophagy [43,44] resulting in dysfunction. To investigate how NAT facilitated ECM remodeling in senescent fibroblasts, eight genes related to energy metabolism, autophagy, and mitophagy were assessed using the RT-qPCR method (Figure 3A). The results indicated that mitophagy-related genes, mitofusin 1 (MFN1) and tensin homologue (PTEN)-induced kinase 1 (PINK1), did not recover following NAT treatment, despite both showing a one-third decrease in ETO-induced senescent fibroblasts (Figure 3B). The

autophagy-associated genes microtubule associated protein 1 light chain 3 alpha (LC3 I) and microtubule associated protein 2 light chain 3 alpha (LC3 II) did not exhibit their usual patterns of change, with these two proteins showing opposite trends (Figure 3B).

Regarding metabolic genes, the glycolysis-related gene PKM1 and the OXPHOS genes mt-ND1 and NADH: ubiquinone oxidoreductase core subunit S1(NDUFS-1), both located on mitochondrial complex I, exhibited contrasting trends in senescent fibroblasts (Figure 3B, 3C). PKM1, the critical enzyme during glycolysis, was upregulated to a 1.2-fold by ETO and subsequently downregulated to nearly 0.6-fold, compared to ETO, following treatment with 2 μM NAT. The gluconeogenic gene, phosphoenolpyruvate carboxykinase 2 (PCK2), which inhibited glycolysis [45], oppositely decreased by 0.6-fold change compared to ETO, however, PCK2 was not upregulated by NAT. In contrast, both mt-ND1 and NDUFS-1 levels significantly declined by one-third in senescent fibroblasts compared with proliferating non-senescent ones. After NAT treatment with 2 μM, mt-ND1 levels recovered to approximately 1.3-fold, while the expression of NDUFS-1 did not improve with NAT. Notably, both two genes were maximumly improved when treated with 2 μM NAT. To further verify the attenuation of glycolysis, PKM1 protein levels were assessed by western blotting. The results indicated that 2 μM NAT significantly downregulated PKM1 protein expression to levels comparable to those in proliferating non-senescent fibroblasts, whereas PKM1 was upregulated to 1.4-fold in senescent fibroblasts (Figure 3D, 3E).

OXPHOS system is embedded in the inner mitochondrial membrane, and is composed of five multiprotein enzyme complexes (I–IV and ATP synthase) and two electron carriers [46]. The mt-ND1 protein is indispensable for mitochondrial respiratory chain complex I assembly and electron transport, providing complex I with NADH dehydrogenase activity [47]. The PKM1 protein participates in the conversion of phosphoenolpyruvate and ADP to pyruvate and ATP during glycolysis, which occurs in the cytoplasm [48]. Comparing to the approximately thirty four molecules of ATP during OXPHOS, glycolysis only produce two molecules of ATP leading to insufficient ATP supplement in senescent cells [9]. According to the entirely opposite trends observed in PKM1 and mt-ND1 between senescent fibroblasts and NAT treated fibroblasts, we postulated that NAT may reprogram the metabolic pattern by shifting glycolysis to OXPHOS, to enhance ATP production during ECM remolding (Figure 3F). Thus, an OCR assay, which reflected the extent of OXPHOS, was conducted, followed by ATP production detection. The significantly improved OCR and ATP production in the NAT treated fibroblasts strongly supported our hypothesis that NAT reprogrammed energy metabolism of senescent fibroblasts, showing a rise of 0.7-fold in OCR and 0.3-fold in ATP production, respectively (Figure 3G, 3H).

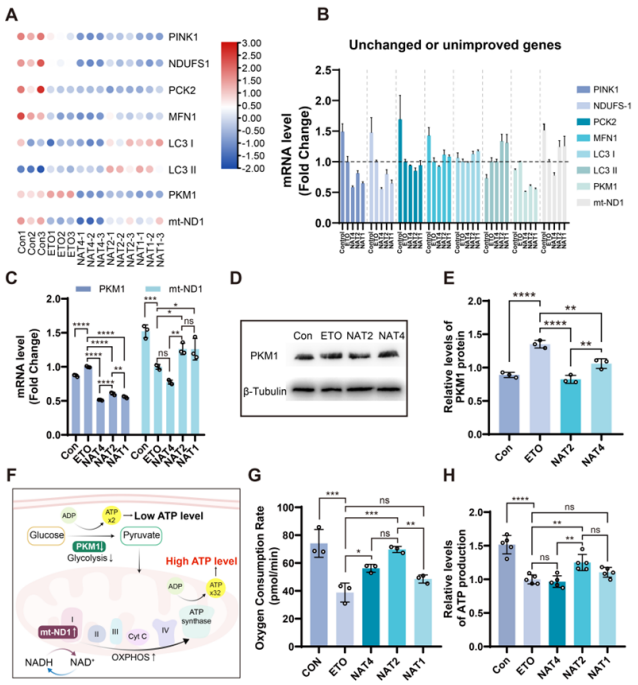

Figure 3. Energy metabolism reprogramming of senescent fibroblasts. (A) Heatmap of relative mRNA expression levels associated with energy metabolism, autophagy and mitophagy, including PINK1, NDUFS1, PCK2, MFN1, LC3 I, LC3 II, PKM1 and mt-ND1, clustered by row scale; (B) Bar chart illustrating the relative levels of gene expression that remained unchanged or unimproved (normalized to gene expressions in ETO group), n=3; (C) Bar chart showing the relative changes in gene expressions that were improved (normalized to gene expressions in ETO group), n=3; (D, E) Western blotting results for PKM1 expression in fibroblasts treated with NAT and quantitative analysis, n=3; (F) Schematic illustration elucidating the relationship between changes in PKM1 and mt-ND1 with oxidative phosphorylation, glycolysis, and subsequent ATP production; (G) OCR detection in senescent fibroblasts, n=3; (H) Relative levels of ATP production, n=5. Data are rep-resented as mean ± SD. *p <0.05, **p < 0.01, ***p < 0.001, ****p < 0.0001, ns, not significant, as determined by one-way ANOVA analyses with Tukey's post-hoc test for all comparisons.

3.3 NAT restored mitochondrial function of senescent fibroblasts

Mitochondria plays an evolving role in energy metabolism and cellular senescence, communicating with the cytosol to keep the balance between the energy demands and energy production by OXPHOS. To investigate whether the alternations of complex I in electron transport chain impaired mitochondrial function, the mitochondrial membrane potential was monitored by JC-1 dye, which shifts from an aggregated form that emits red fluorescence (indicating higher mitochondrial membrane potential) to a monomeric form that emits green fluorescence when the membrane potential declines, which can signal mitochondrial dysfunction [49]. The results indicated a significant decrease of 23.6% in the fluorescent ratio of aggregates to monomers (red/green) in senescent fibroblasts by 23.6% compared to that in proliferating non-senescent fibroblasts, suggesting a decline in membrane potential (Figure 4A, B). Treatment with either NAT4 or NAT2 resulted in an increase in this ratio by 16.7% or 11.1%, respectively, relative to senescent fibroblasts. This indicates an elevated mitochondrial membrane potential achieved through NAT treatment. Moreover, mtROS levels were also effectively downregulated to normal levels after NAT treatments, compared to that in

the positive group (Sox up) (Figure 4C). These results proved that NAT facilitated a restored function of mitochondria in senescent fibroblasts.

The mitochondrial membrane potential formed during electron transportation is essential for ATP production through OXPHOS, while the decreased potential is associated with cellular senescence and apoptosis. Excessive mtROS production usually occurs at complex Ⅰ and complex Ⅲ, primarily due to proton leakage during impaired electron transport chain and abnormal respiratory conditions [50]. Our findings indicated that NAT helped to maintain mitochondrial membrane potential and innocuous mtROS levels in senescent fibroblasts, probably by restoring complex Ⅰ assembly in the electron transport chain.

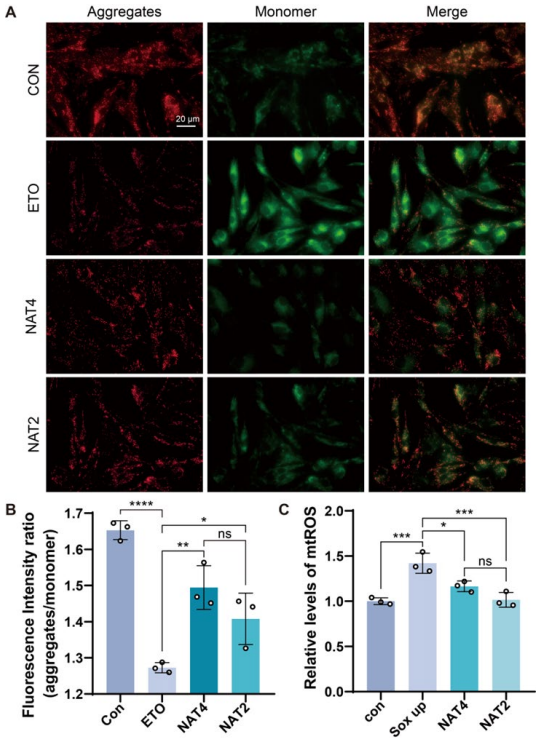

Figure 4. Restoration of Mitochondrial Function in Senescent Fibroblasts. (A) The mitochondrial potential of senescent fibroblasts was assessed by measuring the ratio of JC-1 aggregates (stained red) to JC-1 monomers (stained green), scale bar is 20 μm; (B) Quantitative analysis of fluorescence intensity ratio of aggregates to monomer, n=3; (C) Relative levels of mitochondrial reactive oxygen species (mtROS) were detected using a multimode microplate reader, n=3. Data are represented as mean ± SD. *p <0.05, **p < 0.01, ***p < 0.001, ****p < 0.0001, ns, not significant, as determined by one-way ANOVA analyses with Tukey's post-hoc test for all comparisons. Each image is representative of 3 similar areas.

4. Conclusion

In summary, this study demonstrated that NAT as an NAMPT activator, significantly ameliorated the skin aging both in vitro. NAT reprogrammed the energy metabolism of senescent fibroblasts by attenuating the glycolytic enzyme PKM1 and upregulating the OXPHOS-related protein mt-ND1, contributing to the shift from glycolysis to OXPHOS. This target alteration resulted in the restoration of mitochondrial function, ATP production, and ECM remodeling, consequently leading to the alleviation of skin aging. It would provide the new insight into the anti-aging strategies for the skin.

Conflicts of Interest

No potential conflict of interest was reported by the authors.

References

[1] *López-Otin C, Blasco MA, Partridge L, Serrano M, Kroemer G.* Hallmarks of aging: An expanding universe. Cell. 2023;186:243-278.

[2] *Finkel T.* The metabolic regulation of aging. Nat Med. 2015;21:1416-1423.

[3] *Wiley CD, Campisi J.* From ancient pathways to aging cells—connecting metabolism and cellular senescence. Cell Metabolism. 2016;23:1013-1021.

[4] *Pan C, Locasale JW.* Targeting metabolism to influence aging. Science. 2021;371:234-235.

[5] *Victorelli S, Salmonowicz H, Chapman J, Martini H, Vizioli MG, Riley JS, Cloix C, Hall-Younger E, Espindola-Netto JM, Jurk D, et al.* Apoptotic stress causes mtdna release during senescence and drives the sasp. Nature. 2023;622:627.

[6] *Van deursen JM.* The role of senescent cells in ageing. Nature. 2014;509:439-446.

[7] *Wilson DF.* Oxidative phosphorylation: regulation and role in cellular and tissue metabolism. J Physiol. 2017 Dec 1;595(23):7023-7038.

[8] *Smeitink J, van den Heuvel L, DiMauro S.* The genetics and pathology of oxidative phosphorylation. Nat Rev Genet. 2001 May;2(5):342-52.

[9] *Zhuang Y, Jiang S, Deng X, Lao A, Hua X, Xie Y, Jiang L, Wang X, Lin K.* Energy metabolism as therapeutic target for aged wound repair by engineered extracellular vesicle. Sci Adv. 2024 Apr 12;10(15):eadl0372.

[10] *Wiley CD, Campisi J.* The metabolic roots of senescence: mechanisms and opportunities for intervention. Nat Metab. 2021 Oct;3(10):1290-1301.

[11] *Yu L, Wan Q, Liu Q, Fan Y, Zhou Q, Skowronski AA, Wang S, Shao Z, Liao CY, Ding L, Kennedy BK, Zha S, Que J, LeDuc CA, Sun L, Wang L, Qiang L.* IgG is an aging factor that drives adipose tissue fibrosis and metabolic decline. Cell Metab. 2024 Apr 2;36(4):793-807.e5.

[12] *Zhao X, Psarianos P, Ghoraie LS, Yip K, Goldstein D, Gilbert R, Witterick I, Pang H, Hussain A, Lee JH, Williams J, Bratman SV, Ailles L, Haibe-Kains B, Liu FF.* Metabolic regulation of dermal fibroblasts contributes to skin extracellular matrix homeostasis and fibrosis. Nat Metab. 2019 Jan;1(1):147-157.

[13] *Dou X, Fu Q, Long Q, Liu S, Zou Y, Fu D, Xu Q, Jiang Z, Ren X, Zhang G, Wei X, Li Q, Campisi J, Zhao Y, Sun Y.* PDK4-dependent hypercatabolism and lactate production of senescent cells promotes cancer malignancy. Nat Metab. 2023 Nov;5(11):1887-1910.

[14] *Leng L, Yuan Z, Pan R, Su X, Wang H, Xue J, Zhuang K, Gao J, Chen Z, Lin H, Xie W, Li H, Chen Z, Ren K, Zhang X, Wang W, Jin ZB, Wu S, Wang X, Yuan Z, Xu H, Chow HM, Zhang J.* Microglial hexokinase 2 deficiency increases ATP generation through lipid metabolism leading to β-amyloid clearance. Nat Metab. 2022 Oct;4(10):1287-1305.

[15] *Minhas PS, Latif-Hernandez A, McReynolds MR, Durairaj AS, Wang Q, Rubin A, Joshi AU, He JQ, Gauba E, Liu L, et al.* Restoring metabolism of myeloid cells reverses cognitive decline in ageing. Nature. 2021 Feb;590(7844):122-128.

[16] *Wang JL, Dou XD, Cheng J, Gao MX, Xu GF, Ding W, Ding JH, Li Y, Wang SH, Ji ZW, et al.* Functional screening and rational design of compounds targeting gpr132 to treat diabetes. Nat Metab. 2023;5:1726-1746.

[17] *Waller JM, Maibach HI.* Age and skin structure and function, a quantitative approach (I): blood flow, pH, thickness, and ultrasound echogenicity. Skin Res Technol. 2005 Nov;11(4):221-35.

[18] *Harvell JD, Maibach HI.* Percutaneous absorption and inflammation in aged skin: a review. J Am Acad Dermatol. 1994 Dec;31(6):1015-21.
[19] *Duncan KO, Leffell DJ.* Preoperative assessment of the elderly patient. Dermatol Clin. 1997 Oct;15(4):583-93.
[20] *Farage MA, Miller KW, Elsner P, Maibach HI*. Characteristics of the aging skin. Adv Wound Care (New Rochelle). 2013 Feb;2(1):5-10.
[21] *Choi EH.* Aging of the skin barrier. Clin Dermatol. 2019 Jul-Aug;37(4):336-345.
[22] *Franco AC, Aveleira C, Cavadas C.* Skin senescence: Mechanisms and impact on whole-body aging. Trends Mol Med. 2022;28:97-109.
[23] *Wlaschek M, Maity P, Makrantonaki E, Scharffetter-Kochanek K.* Connective tissue and fibroblast senescence in skin aging. J Invest Dermatol. 2021;141:985-992.
[24] *Bittles AH, Harper N.* Increased glycolysis in ageing cultured human diploid fibroblasts. Biosci Rep. 1984 Sep;4(9):751-6.
[25] *Miwa S, Kashyap S, Chini E, von Zglinicki T.* Mitochondrial dysfunction in cell senescence and aging. J Clin Invest. 2022;132.
[26] *Zwerschke W, Mazurek S, Stöckl P, Hütter E, Eigenbrodt E, Jansen-Dürr P.* Metabolic analysis of senescent human fibroblasts reveals a role for AMP in cellular senescence. Biochem J. 2003 Dec 1;376(Pt 2):403-11.
[27] *Cantó C, Menzies KJ, Auwerx J.* NAD(+) metabolism and the control of energy homeostasis: a balancing act between mitochondria and the nucleus. Cell Metab. 2015 Jul 7;22(1):31-53.
[28] *Adant I, Bird M, Decru B, Windmolders P, Wallays M, de Witte P, Rymen D, Witters P, Vermeersch P, Cassiman D, Ghesquière B.* Pyruvate and uridine rescue the metabolic profile of OXPHOS dysfunction. Mol Metab. 2022 Sep;63:101537.
[29] *Yoshida M, Satoh A, Lin JB, Mills KF, Sasaki Y, Rensing N, Wong M, Apte RS, Imai SI.* Extracellular vesicle-ccontained eNAMPT delays aging and extends lifespan in mice. Cell Metab. 2019 Aug 6;30(2):329-342.e5.
[30] *Jadeja RN, Powell FL, Jones MA, Fuller J, Joseph E, Thounaojam MC, Bartoli M, Martin PM.* Loss of NAMPT in aging retinal pigment epithelium reduces NAD+ availability and promotes cellular senescence. Aging (Albany NY). 2018 Jun 12;10(6):1306-1323.
[31] *Dutta T, Kapoor N, Mathew M, Chakraborty SS, Ward NP, Prieto-Farigua N, Falzone A, DeLany JP, Smith SR, Coen PM, DeNicola GM, Gardell SJ.* Source of nicotinamide governs its metabolic fate in cultured cells, mice, and humans. Cell Rep. 2023 Mar 28;42(3):112218.
[32] *Velma GR, Krider IS, Alves ETM, Courey JM, Laham MS, Thatcher GRJ.* Channeling Nicotinamide Phosphoribosyltransferase (NAMPT) to Address Life and Death. J Med Chem. 2024 Apr 25;67(8):5999-6026.
[33] *Yoshida M, Satoh A, Lin JB, Mills KF, Sasaki Y, Rensing N, Wong M, Apte RS, Imai SI.* Extracellular vesicle-contained enampt delays aging and extends lifespan in mice. Cell Metab. 2019;30:329-342.e325.
[34] *Tan CL, Chin T, Tan CYR, Rovito HA, Quek LS, Oblong JE, Bellanger S.* Nicotinamide metabolism modulates the proliferation/differentiation balance and senescence of human primary keratinocytes. J Invest Dermatol. 2019 Aug;139(8):1638-1647.e3.
[35] *Oblong JE.* The evolving role of the NAD+/nicotinamide metabolome in skin homeostasis, cellular bioenergetics, and aging. DNA Repair (Amst). 2014 Nov;23:59-63.
[36] *Li D, Chen Y, Wang Y, Liu J, Chai L, Zhang Q, Qiu Y, Chen H, Shen N, Shi X, Li M.* NAMPT mediates PDGF-induced pulmonary arterial smooth muscle cell

proliferation by TLR4/NF-κB/PLK4 signaling pathway. Eur J Pharmacol. 2023 Dec 15;961:176151.

[37] *Yao J, Shi Z, Ma X, Xu D, Ming G.* lncRNA GAS5/miR-223/NAMPT axis modulates the cell proliferation and senescence of endothelial progenitor cells through PI3K/AKT signaling. J Cell Biochem. 2019 Sep;120(9):14518-14530.

[38] *Wang SN, Xu TY, Li WL, Miao CY.* Targeting nicotinamide phosphoribosyltransferase as a potential therapeutic strategy to restore adult neurogenesis. CNS Neurosci Ther. 2016 Jun;22(6):431-9.

[39] *Ge B, Wei M, Bao B, Pan Z, Elango J, Wu W.* The role of integrin receptor's α and β subunits of mouse mesenchymal stem cells on the interaction of marine-derived blacktip reef shark (*Carcharhinus melanopterus*) skin collagen. Int J Mol Sci. 2023 May 23;24(11):9110.

[40] *Yamaba H, Haba M, Kunita M, Sakaida T, Tanaka H, Yashiro Y, Nakata S.* Morphological change of skin fibroblasts induced by UV Irradiation is involved in photoaging. Exp Dermatol. 2016 Aug;25 Suppl 3:45-51.

[41] *Shin MH, Rhie GE, Park CH, Kim KH, Cho KH, Eun HC, Chung JH.* Modulation of collagen metabolism by the topical application of dehydroepiandrosterone to human skin. J Invest Dermatol. 2005 Feb;124(2):315-23.

[42] *Zou Z, Long X, Zhao Q, Zheng Y, Song M, Ma S, Jing Y, Wang S, He Y, Esteban CR, Yu N, Huang J, Chan P, Chen T, Izpisua Belmonte JC, Zhang W, Qu J, Liu GH.* A single-cell transcriptomic atlas of human skin aging. Dev Cell. 2021 Feb 8;56(3):383-397.e8.

[43] *Velarde MC, Demaria M, Melov S, Campisi J.* Pleiotropic age-dependent effects of mitochondrial dysfunction on epidermal stem cells. Proc Natl Acad Sci U S A. 2015 Aug 18;112(33):10407-12.

[44] *Jiménez-Loygorri JI, Villarejo-Zori B, Viedma-Poyatos Á, Zapata-Muñoz J, Benítez-Fernández R, Frutos-Lisón MD, Tomás-Barberán FA, Espín JC, Area-Gómez E, Gomez-Duran A, Boya P.* Mitophagy curtails cytosolic mtDNA-dependent activation of cGAS/STING inflammation during aging. Nat Commun. 2024 Jan 27;15(1):830.

[45] *Montal ED, Dewi R, Bhalla K, Ou L, Hwang BJ, Ropell AE, Gordon C, Liu WJ, DeBerardinis RJ, Sudderth J, Twaddel W, Boros LG, Shroyer KR, Duraisamy S, Drapkin R, Powers RS, Rohde JM, Boxer MB, Wong KK, Girnun GD.* PEPCK coordinates the regulation of central carbon metabolism to promote cancer cell growth. Mol Cell. 2015 Nov 19;60(4):571-83.

[46] *Saraste M.* Oxidative phosphorylation at the fin de siècle. Science. 1999;283:1488-1493.

[47] *Lin X, Zhou Y, Xue L.* Mitochondrial complex I subunit MT-ND1 mutations affect disease progression. Heliyon. 2024 Mar 28;10(7):e28808.

[48] *Israelsen WJ, Vander Heiden MG.* Pyruvate kinase: Function, regulation and role in cancer. Semin Cell Dev Biol. 2015;43:43-51.

[49] *Sivandzade F, Bhalerao A, Cucullo L.* Analysis of the mitochondrial membrane potential using the cationic JC-1 dye as a sensitive fluorescent probe. Bio Protoc. 2019 Jan 5;9(1):e3128.

[50] *Chouchani ET, Pell VR, James AM, Work LM, Saeb-Parsy K, Frezza C, Krieg T, Murphy MP.* A unifying mechanism for mitochondrial superoxide production during ischemia-reperfusion injury. Cell Metab. 2016 Feb 9;23(2):254-63.